

PROGRESS IN HIGH POWER HIGH BRIGHTNESS DOUBLE BUNCH SELF-SEEDING AT LCLS-II

A. Halavanau, F.-J. Decker, C. Emma, A. Krasnykh, G. Marcus, A.A. Lutman, Z. Huang, Y. Ding, D. Zhu, J. Krzywinski, A. Ratti, A. Marinelli, C. Pellegrini¹

¹ SLAC National Accelerator Laboratory, Stanford University, Menlo Park CA 94025, USA

Abstract

We have previously shown that we can generate near TW, 15 fs duration, near transform limited X-ray pulses in the 4 to 8 keV photon energy range using the LCLS-II copper linac, two electron bunches, a 4-crystal monochromator/delay line and a fast transverse bunch kicker. The first bunch generates a strong seeding X-ray signal, and the second bunch, initially propagating off-axis, interacts with the seed in a tapered amplifier undulator, where it propagates on axis. In this paper, we investigate the design of the 4-crystal monochromator, acting also as an X-ray delay system, and of the fast kicker, in preparation of the implementation of the system in LCLS-II.

INTRODUCTION

The Double-Bunch FEL (DBFEL) is a method to generate high power and brightness in an X-ray FEL. In this scheme, shown in Fig. 1, the first bunch generates a high power SASE signal, near to saturation value, in the first undulator section and is not used in the second undulator section. The second bunch is seeded at the entrance of the second tapered undulator section by the high power SASE signal, filtered by a four crystals monochromator, also acting as a delay line. A transverse kicker is used to put the second bunch in oscillations around the undulator axis in the first section to avoid lasing. The kick is compensated to propagate the second bunch on axis in the second tapered section.

This concept was first considered to improve the performance of European XFEL and LCLS in Refs [1–3]. The overall design of the DBFEL at LCLS-II has been outlined in [4, 5]. A similar configuration using the second bunch as a fresh bunch with an ultra-fast kicker has been analyzed in the context of self-seeding and harmonic lasing in Ref. [6]. The experimental demonstration of fresh bunch self-seeding in a single bunch was also reported in Ref. [7].

Over the years of LCLS operations, electron beams containing multiple bunches separated by a few RF-buckets have been routinely created in LCLS CuRF linac [8–11]. It was previously demonstrated the DBFEL configuration of LCLS-II HXR undulator gives high peak power and high brightness X-rays in the photon range of 4 to 8 keV [4]. In this proceeding, we provide an update on DBFEL four crystal monochromator design, ultra-fast kicker and XFEL performance.

DBFEL NUMERICAL SIMULATIONS

The LCLS CuRF beamline is simulated using the code elegant [12], to evaluate the effects of the wakefields in the linac and bunch compressors. The particle distribution is

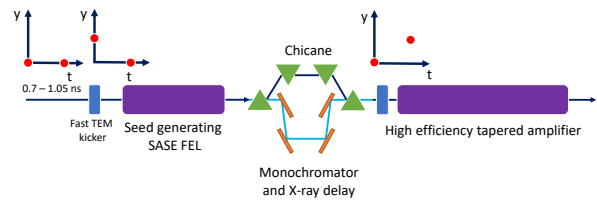


Figure 1: DBFEL schematics: two bunches with 0.7 - 1.05 ns separation are used to generate a high power seed on the second cold bunch at the entrance of the tapered amplifier.

then converted and passed to the FEL code genesis [13] running in time-dependent mode. For tapering studies, we utilize the technique described in [4]. In our simulations, the two bunches are considered to be identical, with 4 kA peak current and 15 fs quasi-flat top profile. We note that optimizing start-to-end beam and optimum taper profile for the amplifier section is a subject of an ongoing study.

FOUR CRYSTAL MONOCHROMATOR

An important part of the DBFEL system is the four crystal monochromator, presented in Fig. 2, that provides narrow bandwidth for double bunch seeding, and matches the delay $\Delta\tau$ between the two bunches. Currently, the monochromator is planned to be installed in the same chicane with the proposed LCLS-II RAFEL project, limiting its horizontal size to $L = 0.67$ cm.

In order to proceed with the design of the four bounce monochromator, let us discuss a few salient parameters of this device. We first start with the location of the monochromator in the undulator beamline. LCLS-II HXR undulator is built with 33 sections, each 3.6 m long, separated by a 0.4 m of free space. Two empty slots at U8 and U15 are available for self-seeding chicane installation.

LCLS-II HXR undulator currently has two empty slots at U8 and U15 locations available for self-seeding chicanes installation. Figure 3 displays gain curves of different photon energies in the SASE section. 4 keV case saturates after 8 undulators, while 8 keV case continues to grow exponentially until U12 location. At the next empty slot at U15 both 4 keV and 8 keV photon energies are saturated. Thus, we conclude that a SASE section of 8 undulators provides more seeding power for DBFEL. We note, that ultimately, experimental electron beam parameters and HXR gain length should be the key factors that determine the location of the DBFEL four crystal monochromator. These measurements are planned shortly after LCLS-II HXR undulator commissioning.

Table 1: C*(111) Parameters in 4-8 keV Photon Energy Range

Parameter	Units	Photon energy	Value
Bragg angle	deg.	4 keV	48.8
Darwin width	μrad	4 keV	69.4
Extinction length	μm	4 keV	2.9
Bandwidth	$\cdot 10^{-5}$	4 keV	6.1
Bragg angle	deg.	8 keV	22.1
Darwin width	μrad	8 keV	24.3
Extinction length	μm	8 keV	5.8
Bandwidth	$\cdot 10^{-5}$	8 keV	6.0

The monochromator uses diamond crystals to provide a narrow bandwidth and avoid complex thermal management [4]. We opt to select C*(111) diamond crystals as the best option for 4-8 keV energy range. C*(111) parameters are given in Tab. 1. The monochromator bandwidth is determined by the Darwin width, which is plotted in Fig. 4. Darwin curves were produced in XOP program [14].

The choice of diamond reflection also defines the geometry of the monochromator via the value of Bragg angle θ . Simple kinematic calculations yield the following equations for monochromator crystals' coordinates. Let us denote the distance between two upper crystals by L . Then the separation between two lower crystals is determined by $\Delta_z = L - c\Delta\tau(\cot^2\theta - 1)/2$, and the lateral displacement by $h = c\Delta\tau/2\tan\theta$. In addition, the bandwidth is defined by $\Delta\omega/\omega = -\Delta\theta/\tan\theta$, where $\Delta\theta$ is the Darwin width. See Fig. 2.

Thus, driven by the space limitations and four crystal geometry, we determine the optimum double bunch separation

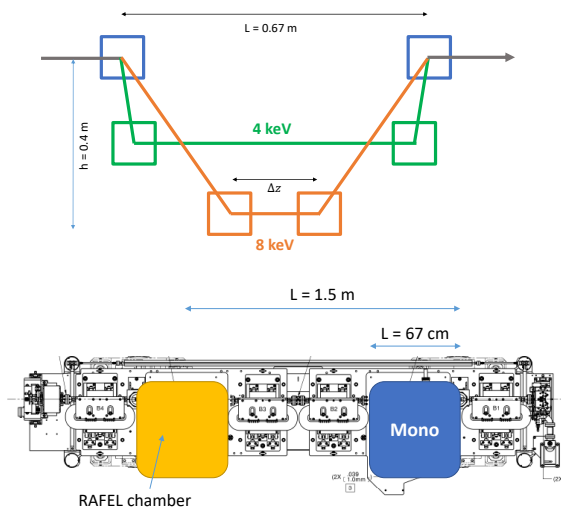


Figure 2: Four crystal monochromator layout (top) and location in the chicane (bottom). Two upper crystals stay fixed, while two lower crystals move in XY plane. See Ref. [15, 16] for the description of the RAFEL project.

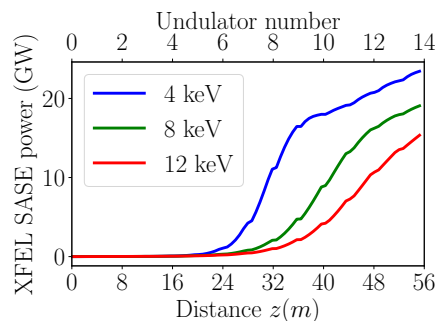


Figure 3: Start-to-end simulation of the SASE section XFEL power as a function of distance for different photon energies.

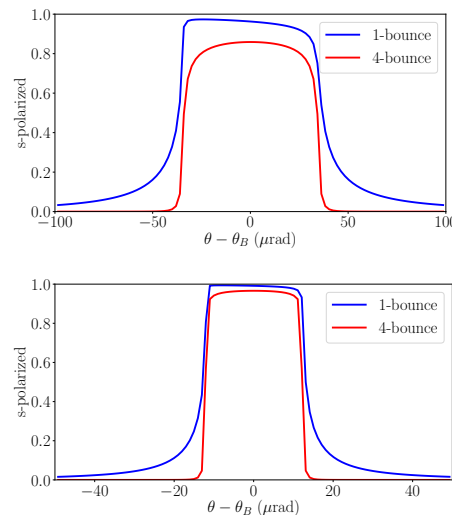


Figure 4: Darwin width of C*(111) 4 keV (top) and 8 keV (bottom) reflections for single and four bounces.

to be 2 RF buckets or $\Delta\tau=0.7$ ns, compared to previously reported number of 3 RF buckets or $\Delta\tau=1.05$ ns. This calculation is summarized in Fig. 5. Alternatively, one can consider the next diamond Bragg reflection of C*(220) to operate at higher photon energies, e.g. up to 12 keV, while reducing the footprint of the monochromator. However, to access 4 keV photons, we consider C*(111) as our primary choice. C*(111) will be procured from Sumitomo Electric and tested at Spring-8 facility in Japan.

We also note the existing nanopositioning stages have a precision of about 20 nm, which translates into about ± 0.2 fs error in total delay time $\Delta\tau$. We estimate the effect of the angular pointing error via $\Delta\tau \sim \Delta\theta/\cos\theta^2$ to be of the order of 1 fs.

ULTRA-FAST KICKER

The performance of the DBFEL system is critically dependent on the ability to control the orbits of two bunches. Initially, first bunch has to propagate on axis in order to provide high power seeding signal. The second bunch has to be put off axis before the SASE section enough to suppress lasing. This will be done with an ultra-fast transverse electromag-

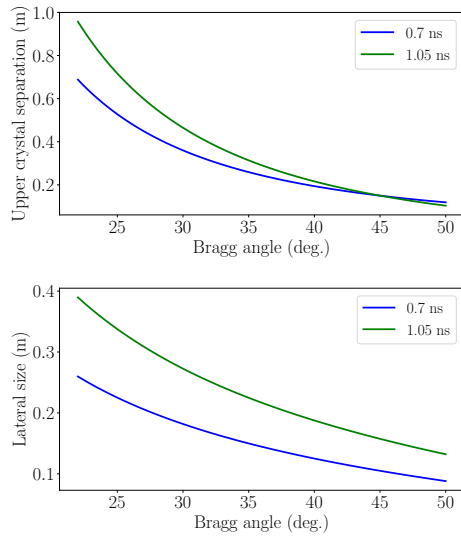


Figure 5: Four crystal monochromator size as a function of Bragg angle for 2 and 3 RF buckets double bunch separation and $\Delta z = 0.15$ m.

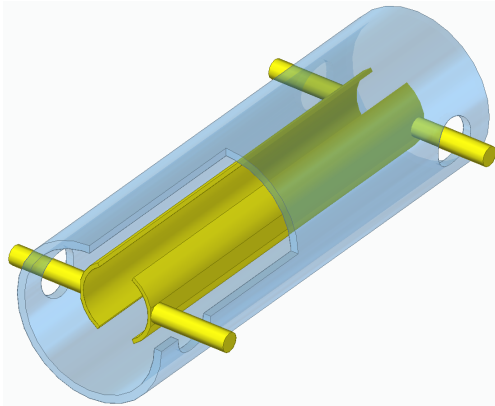


Figure 6: A schematic view of vertical TEM kicker.

netic (TEM) kicker system. Similar kickers were designed for high energy electron beams, including LCLS-II, albeit at larger bunch separations. In the case of DBFEL, bunch separation is about 0.7 ns, approaching the rise time limit of ultra-fast high voltage power supplies. As discussed above, DBFEL can also operate with 1.05 ns or three RF-buckets separation, in case practical implementation of the kicker device does not provide required rise time stability.

The transverse kick required to suppress lasing in the undulators is given by $\theta_C = \sqrt{\lambda/L_g}$, where λ is the radiation wavelength and L_g is the gain length [17]. This value is in the order of 10 μ rad and is translated into about 60 keV/c of transverse momentum at 6 GeV beam energy, thereby determining the required TEM kicker strength. For a TEM structure, kicker strength is given by

$$\alpha = \frac{2VL}{r} \frac{4}{\pi} \sin \frac{\psi}{2}, \quad (1)$$

Table 2: TEM Kicker Specifications

Parameter	Units	Value
Voltage	kV	± 10
Rise time	ns	<0.3
Flat top	ns	3.5 ± 0.5
Pre-pulse	-	$<2\%$
Impedance	Ohm	50

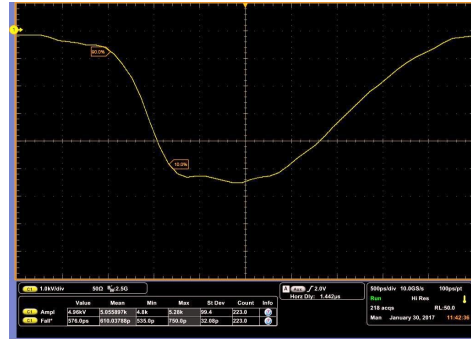


Figure 7: TEM kicker voltage as a function of time.

where $\psi = \pi/3$, V is the voltage, L is the length of the TEM structure, r is the structure radius and ψ is the opening angle [18]. Assuming TEM structure length of about 0.1 m with aperture of 0.01 m, we obtain 3 kV of required voltage.

We then consider a TEM structure, as shown in Fig. 6, with the specifications listed in Tab. 2. In this configuration, high voltage pulse is applied on two vertical plates, filling up TEM structure with EM field collinear with the beam direction. Our initial experiments with pulser prototypes show promising results for 5 kV peak voltage, 0.7 nsec rise time on a 50 Ohm resistive load; see Fig. 7. Pulser power supply design will be based on an employment of drift step recovery processes in semiconductors.

SUMMARY

We have presented the design of two critically DBFEL components: four crystal monochromator and ultra-fast TEM kicker. We concluded that given the limitations of the existing chicane design and CuRF wakefields, the separation of 0.7 ns or two RF-buckets is optimal. This, however, poses a strict constraint on the ultra-fast kicker's rise time. To solve the problem, we consider TEM structure, compatible with existing ultra-fast high voltage power supplies.

ACKNOWLEDGEMENTS

This work was supported by the U.S. Department of Energy Contract No. DE-AC02-76SF00515. The authors are grateful to Y. Feng, H.-D. Nuhn, J. Wu, C. Mayes (SLAC), K.-J. Kim, Y. Shvydko (ANL) for useful discussions.

REFERENCES

- [1] G. Geloni, V. Kocharyan, and E. Saldin, *arXiv, physics.acc-ph:1003.2548*, (2010).

- [2] G. Geloni, V. Kocharyan, and E. Saldin, *arXiv, physics.acc-ph:1207.1981*, (2012).
- [3] Y. Ding, Z. Huang, and R. D. Ruth, *Phys. Rev. ST Accel. Beams*, 13:060703, (2010). doi:10.1103/PhysRevSTAB.13.060703
- [4] A. Halavanau, F.-J. Decker, C. Emma, J. Sheppard, and C. Pellegrini, *Journal of Synchrotron Radiation*, 26(3), (2019). doi:10.1107/S1600577519002492
- [5] A. Halavanau, F.-J. Decker, Y. Ding, C. Emma, Z. Huang, J. Krzywinski, A. A. Lutman, G. Marcus, C. Pellegrini, and D. Zhu, In *Proc. 10th International Particle Accelerator Conference (IPAC2019), Melbourne, Australia, May 19-24, 2019*, paper TUPRB088, 2019. doi:10.18429/JACoW-IPAC2019-TUPRB088
- [6] C. Emma, Y. Feng, D. C. Nguyen, A Ratti, and C. Pellegrini, *Phys. Rev. Acc. and Beams*, 20:030701–10, (2017). doi:10.1103/PhysRevAccelBeams.20.030701
- [7] C. Emma, A. Lutman, M. W. Guetg, J. Krzywinski, A. Marinelli, J. Wu, and C. Pellegrini, *Applied Physics Letters*, 110(15):154101, (2017). doi:10.1063/1.4980092
- [8] F.-J. Decker *et al.*, “A Demonstration of Multi-bunch Operation in the LCLS”, in *Proc. 32nd Int. Free Electron Laser Conf. (FEL’10)*, Malmö, Sweden, Aug. 2010, paper WEPB33, pp. 467–470.
- [9] F.-J. Decker *et al.*, “Two Bunches with ns-Separation with LCLS”, in *Proc. 37th Int. Free Electron Laser Conf. (FEL’15)*, Daejeon, Korea, Aug. 2015, paper WEP023, pp. 634–638.
- [10] F.-J. Decker, K. L. F. Bane, W. S. Colucho, A. A. Lutman, and J. C. Sheppard, “Recent Developments and Plans for Two Bunch Operation with up to 1 μ s Separation at LCLS”, in *Proc. 38th Int. Free Electron Laser Conf. (FEL’17)*, Santa Fe, NM, USA, Aug. 2017, pp. 288–291. doi:10.18429/JACoW-FEL2017-TUP023
- [11] F.-J. Decker *et al.*, “Four X-ray Pulses within 10 ns at LCLS”, in *Proc. 10th Int. Particle Accelerator Conf. (IPAC’19)*, Melbourne, Australia, May 2019, pp. 1859–1862. doi:10.18429/JACoW-IPAC2019-TUPRB086
- [12] M. Borland, “elegant: A Flexible SDDS-Compliant Code for Accelerator Simulation”, APS, LS-287, (2000). doi:10.2172/761286
- [13] S. Reiche, “GENESIS 1.3: a fully 3D time-dependent FEL simulation code”. *Nuclear Instruments and Methods in Physics Research A*, 429:243–248, (1999). doi:10.1016/S0168-9002(99)00114-X
- [14] M. Sanchez del Rio and R. J. Dejus, “Xop v2.4: recent developments of the x-ray optics software toolkit”, *Proc. SPIE*, 8141:8141 – 8141 – 5, (2011). doi:10.1117/12.893911
- [15] G. Marcus *et al.*, Regenerative Amplification for a Hard X-ray Free-Electron Laser. presented at FEL19, Hamburg, Germany, paper TUP032, 2019.
- [16] G. Marcus *et al.*, Regenerative Amplification for a Hard X-ray Free-Electron Laser. presented at FEL19, Hamburg, Germany, paper TUD04, 2019.
- [17] T. Tanaka, H. Kitamura, and T. Shintake, *NIM:A*, 528(1), pp. 172–178, (2004). doi:10.1016/j.nima.2004.04.040
- [18] D. A. Goldberg and G. R. Lambertson, “Dynamic devices. a primer on pickups and kickers”, *AIP Conference Proceedings*, 249(1):537–600, 1992. doi:10.1063/1.41979